


# Enhanced Circular Dichroism via Symmetry Breaking in a Chiral Plasmonic Nanoparticle Oligomer

KHAI Q. LE <sup>1,2,3</sup>

1.—Division of Computational Physics, Institute for Computational Science, Ton Duc Thang University, Ho Chi Minh City, Vietnam. 2.—Faculty of Electrical and Electronics Engineering, Ton Duc Thang University, Ho Chi Minh City, Vietnam. 3.—e-mail: lequangkhai@tdt.edu.vn

A chiral plasmonic nanoparticle oligomer, consisting of four symmetrically arranged nanodisks of different heights and having different optical absorption responses to left and right-handed circularly polarized light illumination, has been experimentally reported in the literature. The resulting circular dichroism (CD) signal was detectable with state of the art CD spectrometers but was much weaker than those of existing chiral nanostructures, i.e., three-dimensional (3-D) chiral metamaterials. In this letter, via symmetry breaking in such an oligomer, the author demonstrates that the CD can be enhanced up to six times compared to that of a symmetric oligomer, and is in the range of a relevant 3-D chiral metamolecule. Through investigation of geometrical parameters including particle size, asymmetric and symmetric gaps, the CD evolution was reported, which provides a useful guideline for design of two-dimensional chiral oligomers adopted as efficient probes for CD spectroscopic applications.

**Key words:** Circular dichroism, chiral plasmonic nanoparticle oligomer, symmetry breaking

## INTRODUCTION

Chiral molecules exhibiting circular dichroism (CD) properties are able to absorb different amounts of left-handed circularly polarized (LCP) and right-handed circularly polarized (RCP) incident light. They have been used in various applications associated with pharmaceuticals,<sup>1</sup> biochemistry,<sup>2</sup> and electromagnetics.<sup>3</sup> Natural chiral molecules usually exhibit weak optical CD signals. Research in optical chirality attempts to design molecules with stronger CD properties, and has led to the realization of artificial chiral nanostructures.<sup>4</sup> Numerous chiral nanostructures, including chiral nanoantennas,<sup>5</sup> metamaterials,<sup>6</sup> colloidal chiral nanoparticles,<sup>7</sup> and many others,<sup>8</sup> have been reported theoretically and experimentally. Closely packed chiral plasmonic nanoparticle assemblies such as clusters and oligomers can induce optical chirality. The

induced chiral optical (known as chiroptical) effect that can be significantly enhanced by plasmonic resonances related to electric and magnetic fields, and resonances associated with the spatial geometry of the nanostructures such as Fano-type resonances,<sup>9</sup> are of emerging interest in various fields including the chirality detection of biomolecules. The chirality detection sensitivity of biomolecules when interacting with planar chiral plasmonic nanostructures can be significantly improved thanks to such chiroptical effects.<sup>10</sup>

Planar chiral metamaterials have recently attracted interest for on-chip molecular chirality detection applications owing to their nonbulky geometry. Chiral plasmonic metamaterials consisting of four symmetrically arranged nanoparticles have been recently reported in Ref. 11. Thanks to the colloidal lithography technique, engineered metal nanodisks of different heights could be precisely positioned in a chiral nanoparticle oligomer. However, its CD is relatively weak due to its in-plane symmetric geometry. In this work, the author

proposes symmetry breaking in such a symmetric oligomer as a route towards enhancement of the CD. Symmetry breaking increases the degree of spatial geometry of the nanostructure that may, in turn, improve the chiroptical effect. The resulting CD ( $16058 \text{ nm}^2$ ) is approximately six times stronger than that of the symmetric oligomer ( $2798 \text{ nm}^2$ ), and is even a bit higher than that of three-dimensional (3-D) chiral metamolecules ( $14,500 \text{ nm}^2$ ).<sup>9</sup>

### CHIRAL PLASMONIC NANOSTRUCTURES AND MODELLING METHOD

A schematic of two chiral nanoparticle oligomers with opposite handedness labeled as LH and RH are depicted in Fig. 1. Each oligomer consists of four closely packed gold nanodisks of the same diameter  $d$  but different heights and separated by interparticle gaps. When the asymmetric gap ( $ag$ ) between two particles (numbers 3 and 4 in Fig. 1) is equal to the gap ( $g$ ) between the other two neighboring particles (numbers 1 and 4 in Fig. 1), we obtain a symmetric oligomer. In contrast, when  $ag$  is larger than  $g$ , an asymmetric oligomer is obtained. All the nanoparticle oligomers were deposited on a glass substrate with refractive index  $n = 1.5$ .

In this work, CD is defined as the difference between the extinction cross-sections (ECS) of an oligomer under LCP and RCP light illumination. In order to compute the ECS of an oligomer, the author has numerically solved the chiral light-matter interaction problem via the full-wave Maxwell's equations solver based on the boundary element method that is implemented in the MATLAB-based toolbox MNPBEM.<sup>12</sup> The complex refractive index of Au with realistic material losses was extracted from experimental data.<sup>13</sup>

### RESULTS AND DISCUSSION

The calculated ECSs of the symmetric oligomers for both left and right handedness under LCP and RCP light incidence are shown in Fig. 2a and b. The symmetric oligomer consists of four nanodisks of the same diameter  $d = 80 \text{ nm}$ . The interparticle gaps are identical with  $ag = g = 10 \text{ nm}$ . The heights of the designated particles (numbers 1, 2, 3, and 4) are  $40 \text{ nm}$ ,  $60 \text{ nm}$ ,  $30 \text{ nm}$ , and  $10 \text{ nm}$ , respectively. Such differences in height of the individual nanoparticles induce optical activities in the whole oligomer. As a consequence, the symmetric chiral oligomers exhibit different extinction responses to the handedness of the incident chiral light.

For the left-handed (LH) oligomer, the LCP-ECS spectrum exhibits two resonant peaks with maxima at approximately  $663 \text{ nm}$  and  $727 \text{ nm}$ , as seen in Fig. 2a. The RCP-ECS spectrum exhibits resonant peaks at the same wavelengths but of different magnitudes. While the resonant peak at  $663 \text{ nm}$  in the LCP-ECS spectrum has a larger magnitude than that of the corresponding peak in the RCP-ECS spectrum, the resonant peak at  $727 \text{ nm}$  in the LCP-ECS spectrum has a smaller magnitude than that of the corresponding peak in the RCP-ECS spectrum. The slight discrepancy of these ECS spectra results in the CD activity of the symmetric chiral oligomer as shown in Fig. 2c. These optical extinction responses are reversed for the opposite handedness of the oligomer, as seen in Fig. 2b. Thus, the CD of the right-handed (RH) oligomer is a mirror image of that of the LH oligomer, as seen in Fig. 2c.

However, the CD of the symmetric chiral oligomer is relatively weak. Symmetry breaking in such a symmetric oligomer by increasing the asymmetric gap  $ag$  leads to a significant enhancement of the CD of the symmetry-broken oligomer. Symmetry

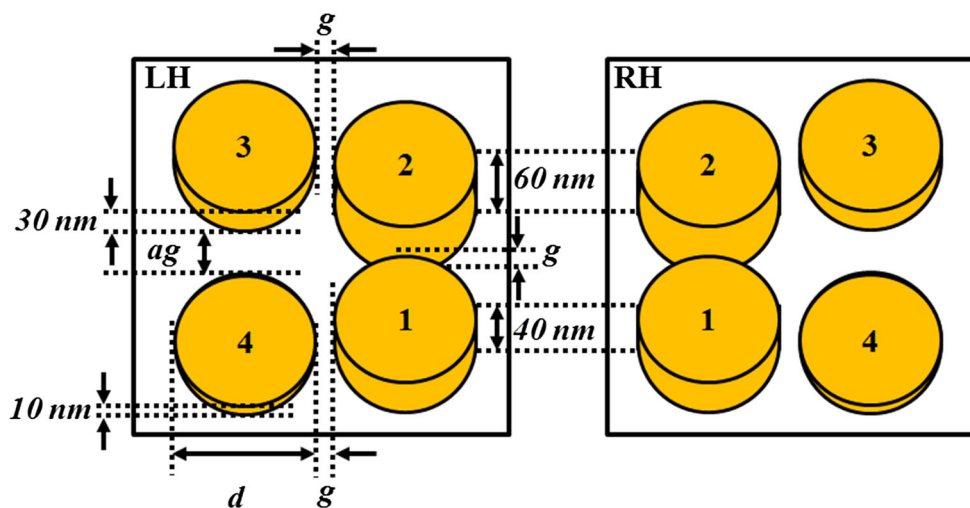


Fig. 1. Chiral plasmonic nanoparticle oligomers. Schematic of chiral plasmonic nanoparticle oligomers with opposite handedness. All the nanoparticles have the same diameter but are of different heights.

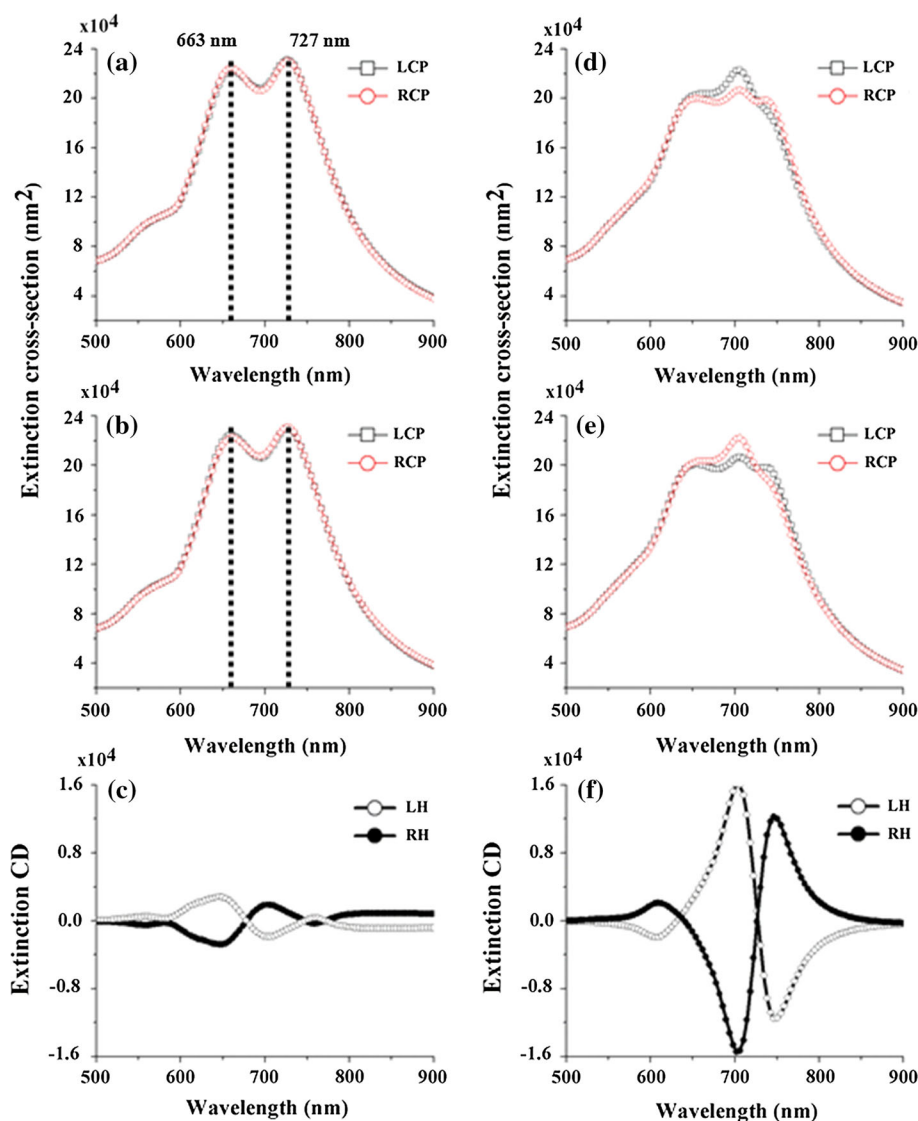


Fig. 2. Symmetric versus asymmetric chiral oligomers' spectral responses. Extinction cross-sections (a–e) of symmetric and asymmetric chiral oligomers with opposite handedness under LCP and RCP light illumination. (c and f) CD of symmetric and asymmetric chiral oligomers with LH and RH handedness.

breaking in nanoparticle oligomers or clusters was reported to induce plasmonic resonances related to electric and magnetic fields, and resonances associated with the spatial geometry of the oligomer, i.e., Fano resonances.<sup>9,14</sup> This study reveals clear differences between the ECSs of the symmetry-broken oligomers for both left and right-handedness under LCP and RCP light illumination, as seen in Fig. 2d and e. Such differences result in a strong CD of the asymmetric oligomer as seen in Fig. 2f. A comparison of the CD of the symmetric oligomer shown in Fig. 2c and that of the asymmetric oligomer shown in Fig. 2f reveals that the latter ( $16,058 \text{ nm}^2$ ) is approximately six times stronger than the former ( $2798 \text{ nm}^2$ ), and is in the range of relevant 3-D chiral metamolecules ( $14,500 \text{ nm}^2$ ).<sup>9</sup> Symmetry breaking in the oligomer increases the degree of

its spatial geometry that, in turn, results in an enhancement of the CD. It appears that the 2-D asymmetric oligomer provides a relevant or even higher CD than that of the 3-D chiral metamolecules. Furthermore, the fabrication of such a 2-D oligomer is much easier than the 3-D metamolecules, especially for large scale productions, which offers an alternative nanomaterial as an efficient probe for CD spectrometer.

Figure 3 shows the CD spectra of asymmetric oligomers for different asymmetric gaps  $ag$ . It is evident that the CD increases with an increase in the asymmetric gap. When the asymmetric gap ( $ag = 5 \text{ nm}$ ) is less than the symmetric gap ( $g = 10 \text{ nm}$ ), the CD decreases since the symmetry breaking is small. In contrast, when the gap between the other two neighboring nanoparticles

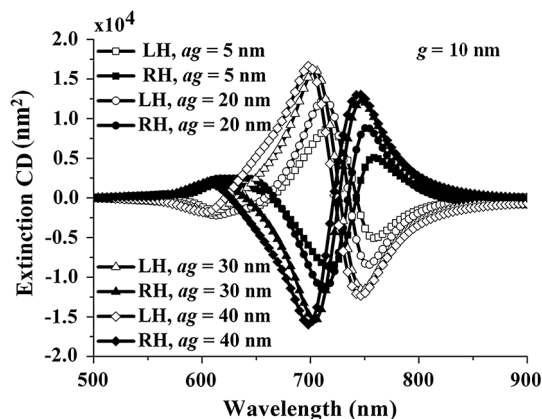


Fig. 3. CD signal of asymmetric chiral oligomers for various asymmetric gaps. CD spectra of two LH and RH chiral oligomers for various asymmetric gaps ( $ag$ ). The heights of the designated particles (numbers 1, 2, 3, and 4) are 40 nm, 60 nm, 30 nm, and 10 nm, respectively. All the particles have the same diameter  $d = 80$  nm. The interparticle gap of the other two neighboring nanoparticles  $g$  was fixed at 10 nm.

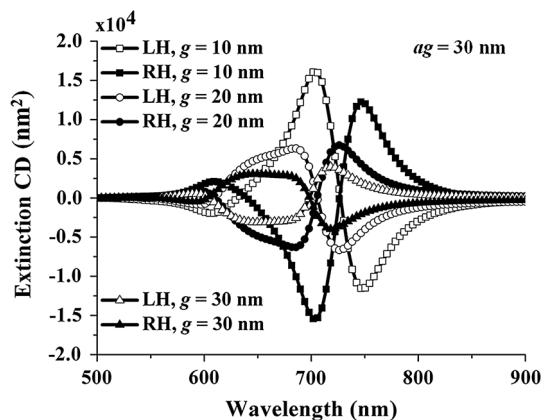


Fig. 4. CD spectra of asymmetric chiral oligomers for various symmetric gaps. CD spectra of symmetry-broken oligomers for both left and right-handedness for different symmetric gaps ( $g$ ). The geometrical parameters of the oligomers are the same as those in Fig. 3 with the asymmetric gap  $ag = 30$  nm.

increases, the CD decreases, since the mutual coupling of the neighboring nanoparticles is decreased, as seen in Fig. 4.

Figure 5 shows the CD spectra of asymmetric oligomers for different particle diameters  $d$ . An increase in the size of the nanoparticle results in a redshift of the plasmonic resonances in the extinction and CD spectra. As the nanoparticle size increases, the oscillation path of the electric charges in the particle increases, leading to a decrease of the free electron relaxation rate. It results in the free electron energy decrease in resonance with the frequency of the incident light.<sup>15</sup> In addition, the magnitude of the CD also increases as the particle diameter is increased. The strong CD properties of the symmetry-broken oligomer may induce strong chiroptical effects that have potential for many

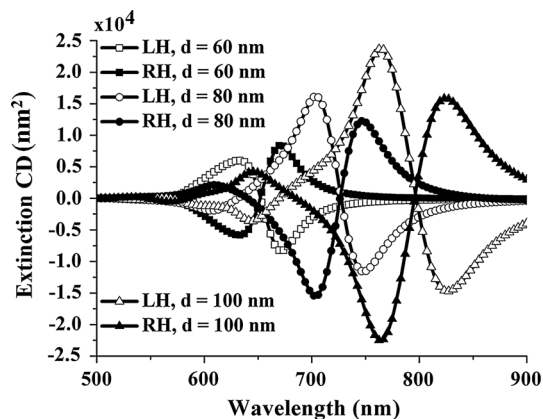


Fig. 5. Asymmetric chiral oligomers with respect to nanoparticle diameters. CD spectra of symmetry-broken oligomers for both left and right-handedness for different particle diameters ( $d$ ). The geometrical parameters of the oligomers are the same as those in Fig. 3 with the gaps  $ag = 30$  nm and  $g = 10$  nm.

applications, especially in the chirality detection of biomolecules.

## CONCLUSIONS

A chiral plasmonic nanoparticle oligomer consisting of four asymmetrically arranged Au nanodisks, and exhibiting stronger CD than that of the symmetric counterpart, has been introduced in this paper. Symmetry breaking causes an increase in the degree of spatial geometry of the oligomer thereby resulting in an enhancement of the CD. The amplification of the CD signal definitely benefits applications related to the chiral light matter interaction.

## ACKNOWLEDGEMENTS

This research is funded by Vietnam National Foundation for Science and Technology Development (NAFOSTED) under Grant Number “103.03-2017.32”.

## REFERENCES

1. L.A. Nguyen, H. He, and C. Pham-Huy, *Int. J. Biomed. Sci.* 2, 85 (2006).
2. N. Berova, K. Nakanishi, and R.W. Woody, *Circular Dichroism: Principles and Applications* (New York: VCH, 1994).
3. J.B. Pendry, *Science* 306, 1353 (2004).
4. A.D. Falco, *Nat. Mater.* 13, 846 (2014).
5. N. Meinzer, E. Hendry, and W.L. Barnes, *Phys. Rev. B* 88, 041407(R) (2013).
6. S.S. Oh and O. Hess, *Nano Converg.* 2, 24 (2015).
7. T. Yasukawa, H. Miyamura, and S. Kobayashi, *Chem. Soc. Rev.* 43, 1450 (2014).
8. S.J. Yoo and Q.-H. Park, *Phys. Rev. Lett.* 114, 203003 (2015).
9. K.Q. Le, *J. Electron. Mater.* (2017). <https://doi.org/10.1007/s11664-017-5644-0>.
10. E. Hendry, T. Carpy, J. Johnston, M. Popland, R.V. Mikhaylovskiy, A.J. Laphorn, S.M. Kelly, L.D. Barron, N. Gadegaard, and M. Kadodwala, *Nat. Nanotechnol.* 5, 783 (2010).
11. R. Ogier, Y. Fang, M. Svedendahl, P. Johansson, and M. Käll, *ACS Photon.* 1, 1074 (2014).

12. U. Hohenester and A. Trügler, *Comput. Phys. Commun.* 183, 370 (2012).
13. J.B. Johnson and R.W. Christy, *Phys. Rev. B* 6, 4370 (1972).
14. F. Shafiei, F. Monticone, K.Q. Le, X.X. Liu, T. Hartsfield, A. Alù, and X. Li, *Nat. Nanotechnol.* 8, 95 (2013).
15. V. Amendola, R. Pilot, M. Frasconi, O.M. Marago, and M.A. Lati, *J. Phys. Condens. Matter* 29, 203002 (2017).